Hydrolysis–Condensation Process of β-Diketonates-Modified Cerium(IV) Isopropoxide

François Ribot, Paul Toledano, and Clément Sanchez*

Laboratoire de Chimie de la Matière Condensée, URA 302, Université P. et M. Curie, 4, place Jussieu, 75252 Paris Cedex, France

Received November 26, 1990. Revised Manuscript Received May 13, 1991

Acetylacetone-modified cerium(IV) isopropoxide precursors have been synthesized and structurally characterized by means of IR and EXAFS analyses. Their hydrolysis yields colloidal dispersions and gels. The morphology of these materials was analyzed with X-ray and light-scattering techniques. The complexation ratio acac/Ce = x (acac = acetylacetonato) is a key parameter for the system. Within the complexation range x = 0–2, hydrolysis of acetylacetone-modified precursors leads to three different domains. For $x < 0.15$, hydrolysis leads to precipitation. For $0.15 \leq x < 1$, sols are obtained. The mean hydrodynamic diameter of the particles can be modulated from 450 to ≈15 Å when x goes from 0.15 to 1.0. These sols slowly turn into gels even for cerium concentrations as low as 0.05 M. For $1 \leq x \leq 2$, small oligomeric species are formed and remain stable without any gelation. A simple model is proposed to account for the size control. It is based on the variation of the functionality of the precursor, which comes from the fact that acetylacetonato ligands are not removed upon hydrolysis. Other studies on acetylacetone-modified metal alkoxides show that this model can be generalized.

Introduction

Sol–gel processing has gained scientific interest during the past 10 years.[1-13] A careful control of such chemistry allows the formation of better or even new materials. Narrow size distribution powders of controlled morphology can be obtained from colloids,[14] and ceramic fibers or coating can be easily made by taking advantage of the rheological properties of gels. Most of the basic studies have been carried out on the sol-gel alkoxide processing of SiO_2-, Al_2O_3-, TiO_2-, and ZrO_2-based ceramics.[1-13] The use of acetylacetone has already been shown to be of great value in improving the sol–gel processing of metal alkoxides.[15] Stable TiO_2-based colloids have been prepared from $Ti(OPr^i)_3(acac)$.[16] Spheroidal particles of zirconia, with narrow size distribution, can be precipitated from acetylacetone-modified $Zr(OPr^i)_4$. The size of the solid particles is strongly correlated to the acac/Zr ratio.[17] Monolithic gels can be prepared by hydrolysis of $Zr(OPr^n)_4$ with acetylacetone and acid catalysis.[18,19] More recently, zirconia fibers were made from $Zr(OPr^n)_4$ modified with acetylacetone.[20]

However, practically no papers can be found in the literature about cerium oxide gels or colloids synthesized via hydrolysis of cerium(IV) alkoxide precursors. Cerium oxide derived systems show interesting applications in various areas such as catalysis,[21] optical additives,[22] ionic conduction, and counter electrodes for electrochromic devices.[23,24]

Cerium(IV) isopropoxide is a very moisture sensitive compound. Its hydrolysis performed under basic, acid, or neutral conditions yields precipitates. Spontaneous precipitation can be avoided by using acetylacetone-modified precursors. This paper reports the sol–gel synthesis and characterization of cerium oxide based gels and colloids obtained via hydrolysis of modified $Ce(OPr^i)_{4-x}(acac)_x$ ($0.15 < x < 1.0$). All of the different steps from the cerium alkoxide precursors up to the gels have been studied. The different chemical species involved during the sol–gel synthesis have been characterized by IR and extended X-ray absorption fine structure (EXAFS). Shape and particle growth have been followed by scattering techniques; i.e., small-angle X-rays scattering (SAXS) and quasielastic light scattering (QELS).

Experimental Section

Cerium(IV) isopropoxide was synthesized according to the procedure described by Gradeff et al.[25] All experiments were performed under dry argon with Shlenk-line techniques to avoid any partial hydrolysis by atmospheric moisture. Purification was done by crystallization of $Ce_2(OPr^i)_8 \cdot 2HOPr^i$ from anhydrous isopropyl alcohol.

(1) Zelinsky, B. J. J.; Uhlmann, D. R. *J. Phys. Chem. Solids* **1984**, *45*, 1069.
(2) Livage, J.; Sanchez, C.; Henry, M.; Doeuff, S. *Solid State Ionics* **1989**, *32/33*, 633.
(3) Schmidt, H. *J. Non-Cryst. Solids* **1988**, *100*, 51.
(4) Ulrich, D. R. *J. Non-Cryst. Solids* **1988**, *100*, 174.
(5) Nabavi, M.; Doeuff, S.; Sanchez, C.; Livage, J. *J. Non-Cryst. Solids* **1990**, *121*, 31.
(6) Sanchez, C.; Babonneau, F.; Doeuff, S.; Leaustic, A. In *Ultrastructure Processing of Advanced Ceramics*; Mackenzie, J. D., Ulrich, D. R., Eds.; Wiley: New York, 1988; p 77.
(7) Sakka, S.; Kozuka, H.; Kim, S. H. In *Ultrastructure Processing of Advanced Ceramics*; Mackenzie, J. D., Ulrich, D. R., Eds.; Wiley: New York, 1988; p 161.
(8) Pouxviel, J. C.; Biolot, J. P. In *Ultrastructure Processing of Advanced Ceramics*; Mackenzie, J. D., Ulrich, D. R., Eds.; Wiley: New York, 1988; p 197.
(9) Hench, L.; Orcel, G.; Nogues, J. L. In *Better Ceramics Through Chemistry II*; Brinker, C. J., Clark, D. E., Ulrich, D. R., Eds.; MRS: Pittsburgh, 1986; p 35.
(10) Klemperer, W. G.; Mainz, V. V.; Ramamurthi, S. D.; Rosenberg, F. S. In *Better Ceramics Through Chemistry III*; Brinker, C. J., Clark, D. E., Ulrich, D. R., Eds.; MRS: Pittsburgh, 1988; p 15.
(11) Hubert-Pfalzgraf, L. G.; Poncelet, O.; Daran, J. C. In *Better Ceramics Through Chemistry IV*; Zelinski, B. J. J., Brinker, C. J., Clark, D. E., Ulrich, D. R., Eds.; MRS: Pittsburgh, 1990; p 73.
(12) Hurd, A. J.; Brinker, C. J. In *Better Ceramics Through Chemistry IV*; Zelinski, B. J. J., Brinker, C. J., Clark, D. E., Ulrich, D. R., Eds.; MRS: Pittsburgh, 1990; p 575.
(13) Brinker, C. J.; Scherrer, G. W. *Sol–Gel Science: The Physics and Chemistry of Sol–Gel Processing*; Academic Press: New York, 1990.
(14) Matijevic, E. *Acc. Chem. Res.* **1981**, *14*, 22.
(15) Mehrotra, R. C.; Bohra, R.; Gaur, D. P. *Metal β-Diketonates and Allied Derivatives*; Academic Press: London, 1978.
(16) Leaustic, A.; Babonneau, B.; Livage, J. *Chem. Mater.* **1989**, *1*, 248.
(17) Rinn, G.; Schmidt, H. In *Ceramic powder science II.A, 1*; Messing, G. L., Fuller Jr., E. R., Hausner, H., Eds.; The American Ceramic Society: Westerville, OH, 1988; p 23.
(18) Debsikdar, J. C. *J. Non-Cryst. Solids* **1986**, *86*, 231.
(19) Papet, P.; Le Bars, N.; Baumard, J. F.; Lecomte, A.; Dauger, A. *J. Mater. Sci.* **1989**, *24*, 3850.
(20) De, G.; Chatterjee, A.; Ganguli, D. *J. Mater. Sci. Lett.* **1990**, *9*, 845.
(21) Fierro, J. L. G.; Mendioroz, S.; Olivani, A. M. *J. Colloids Interface Sci.* **1985**, *107*, 60.
(22) Maestro, P. *J. Less Comm. Met.* **1985**, *111*, 43.
(23) Sarkar, P.; Nicholson, P. S. *Solid State Ionics* **1986**, *21*, 49.
(24) Baudry, P.; Rodrigues, A. C. M.; Aegerter, M. A.; Bulhoes, L. O. *J. Non-Cryst. Solids* **1990**, *121*, 319.
(25) Gradeff, P. S.; Screiber, F. G.; Mauermann, H. *J. Less Comm. Met.* **1986**, *126*, 335.

0897-4756/91/2803-0759$02.50/0

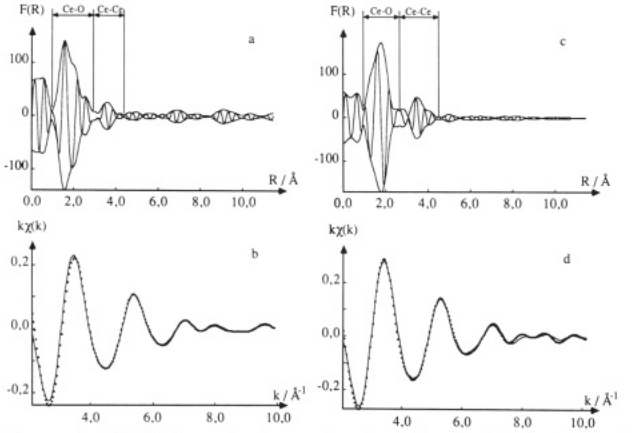

Figure 1. EXAFS results for cerium L_{III} edge. (a) Experimental Fourier transform for $Ce(OPr^i)_4$ in isopropyl alcohol. (b) Filtered EXAFS signal (···) and simulation for $Ce(OPr^i)_4$ in isopropyl alcohol. (c) Experimental Fourier transform for $Ce(OPr^i)_{3.5}(acac)_{0.5}$ in isopropyl alcohol. (d) Filtered EXAFS signal (···) and simulation for $Ce(OPr^i)_{3.5}(acac)_{0.5}$ in isopropyl alcohol.

Complexation was performed by direct addition to a precursor solution of the proper volume of acetylacetone diluted in isopropyl alcohol (10% acacH). Such a procedure minimizes local overconcentration, which favors formation of cerium tetrakis(acetylacetonate). Molar ratios of acac/Ce were investigated between 0 and 2. The reaction produced a color change from yellow to red, which qualitatively indicates the interaction between acetylacetone and cerium. The overall reaction can be written[26]

$$Ce(OPr^i)_4 + x\text{acacH} \rightarrow Ce(OPr^i)_{4-x}(acac)_x + x\text{HOPr}^i$$

Hydrolysis was performed under magnetic stirring with a 10% water–isopropyl alcohol mixture. The H_2O/Ce molar ratio was kept at 10 for all the experiments.

Xerogels were obtained by vacuum drying of the colloidal suspension at 70 °C.

Infrared absorption spectra were recorded on a 783 Perkin-Elmer spectrometer over the 4000–400-cm^{-1} region, by using solutions in carbon tetrachloride between two ZnSe disks.

EXAFS spectra were recorded at the cerium L_{III} edge (5723.4 eV) at LURE (Orsay, France) by using the EXAFS IV (1.85 GeV) spectrometer equipped with a two-crystal Si(111) monochromator and mirrors for harmonics removal. Energy was scanned by 2-eV steps over the range 5600–6200 eV. Background absorption was computed from the pre-edge region (Victoreen approximation) and subtracted from the spectra. Atomic absorption was approximated with a fourth-degree polynomial. The energy reference for calculation of the wave vector scale was taken at the maximum of the absorption. EXAFS signals were extracted according to the Lengeler–Eisenberger formula.[27] EXAFS modulations were analyzed by using standard methods based on single scattering theory.[27,28] The Fourier transform of the signals was computed between 2 and 10 $Å^{-1}$ with a Kaiser truncation window ($\tau = 1.5$). Only the modulations corresponding to peaks between 1 and 4.5 Å on the Fourier transforms (filtered EXAFS signal) were taken into account for simulation and fitting procedures.[28] Amplitude and phase shift functions were taken from McKale tables.[29] The mean free path of the photoelectron was varied linearly with the wave vector ($\lambda = 2k$).

Quasielastic light-scattering measurements were carried out with a He–Ne laser using a Brookhaven BI2030AT photocorrelator and a Amtec photogoniometer. Scattered intensity was adjusted, if necessary, by dilution of the sample with anhydrous isopropyl alcohol. Analysis of the different moments of the correlation function was used to determine the mean diffusion coefficient (D_T) of the particles. The mean hydrodynamic diameter was then computed with the Stoke–Einstein equation.

Small-angle X-ray scattering experiments were performed at LURE (Orsay, France) using the D22 spectrometer. The distance sample to detector (1.14 m) and the wavelength (1.28 Å) gave a Q domain ranging from 6.3×10^{-3} to 2.3×10^{-1} $Å^{-1}$. The scattered intensity was corrected for solvent (isopropyl alcohol) background scattering.

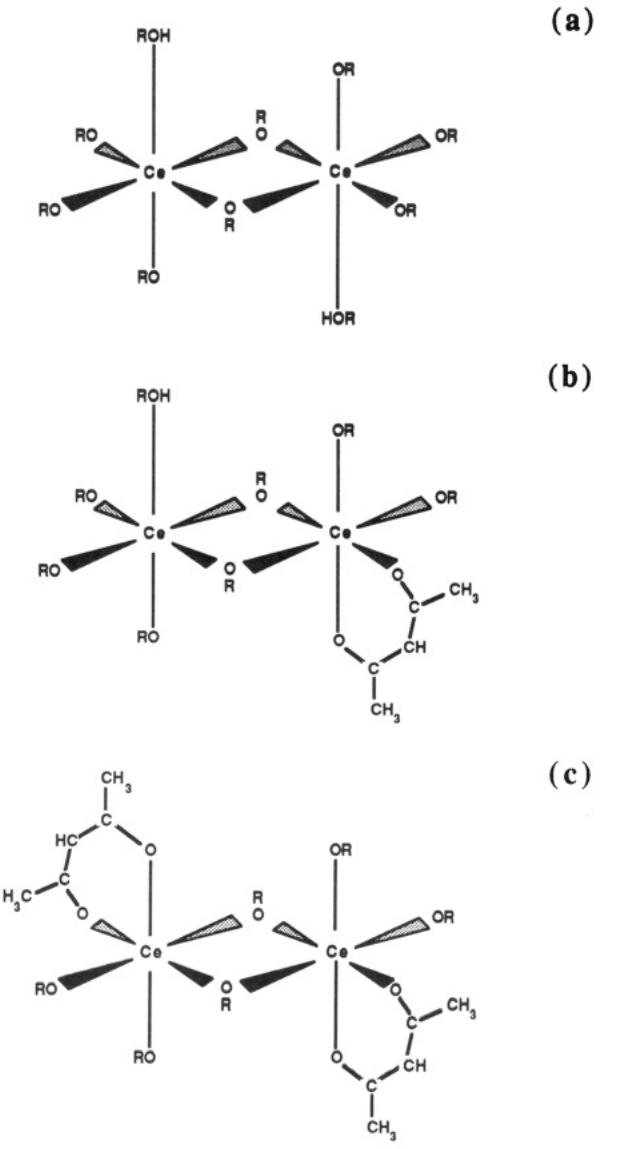

Figure 2. Schematic representations of the proposed dimeric structures for (a) $Ce(OPr^i)_4$ in isopropyl alcohol $[Ce_2(OPr^i)_8 \cdot 2HOPr^i]$, (b) $Ce(OPr^i)_{3.5}(acac)_{0.5}$ in isopropyl alcohol $[Ce_2(OPr^i)_7(acac) \cdot HOPr^i]$, and (c) $Ce(OPr^i)_3(acac)$ in isopropyl alcohol $[Ce_2(OPr^i)_6(acac)_2 \cdot 2HOPr^i]$.

Results and Discussion

Cerium(IV) Isopropoxide. The Fourier transform of the EXAFS signal of $Ce(OPr^i)_4$ in isopropyl alcohol is shown in Figure 1a. The filtered EXAFS signal and simulation are shown in Figure 1b. The best fit (1.2%) was obtained with three Ce–O shells and one Ce–Ce shell. The numbers of neighbors (N), the distances (R), and the Debye–Waller factors (σ) are listed in Table I. The cerium shell shows the existence of oligomeric species. Previous ebulliometric experiments performed in isopropyl alcohol were consistent with the presence of dimeric species in equilibrium with a small amount of monomers (<10%).[30] Moreover the presence in isopropyl alcohol solution of

(26) Mehrotra, R. C.; Misra, T. N.; Misra, S. N. *Indian J. Chem.* **1965**, *3*, 525.
(27) Teo, B. K. *EXAFS: Basic Principles and Data Analysis*; Springer-Verlag: Berlin, 1986.
(28) Michalowicz, A. *Structures fines d'absorption en chimie Logiciels d'analyse: EXAFS pour le MAC*; Verdaguer, M., Dexpert, H., Eds.; Ecole d'été du CNRS: Garchy, 1988; Vol 3(1).
(29) McKale, A. G. *J. Am. Chem. Soc.* **1988**, *110*, 3763.

Table I. Number of Neighbors, Distance, and Debye-Waller Factors Obtained from Cerium L_{III} Edge EXAFS Experiments

compound	shell	N	R, Å	σ, Å^2	fit, %
$Ce(OPr^i)_4$ in $HOPr^i$	Ce–O	2	2.13	0.066	1.2
	Ce–O	3	2.32	0.087	
	Ce–O	1	2.82	0.084	
	Ce–Ce	0.6	3.78	0.085	
$Ce(OPr^i)_{3.5}(acac)_{0.5}$ in $HOPr^i$	Ce–O	2	2.16	0.088	0.8
	Ce–O	3.5	2.32	0.100	
	Ce–O	0.5	2.79	0.033	
	Ce–Ce	1	3.69	0.080	
$Ce(OPr^i)_3(acac)$ in $HOPr^i$	Ce–O	2	2.18	0.091	0.5
	Ce–O	4	2.31	0.097	
	Ce–O	1	2.70	0.091	
	Ce–Ce	1	3.71	0.085	
"$Ce(OPr^i)_{3.5}(acac)_{0.5}\cdot 10H_2O$" in $HOPr^i$	Ce–O	5.8	2.27	0.110	1.0
	Ce–O	1.4	2.68	0.110	
	Ce–Ce	1.2	3.80	0.066	

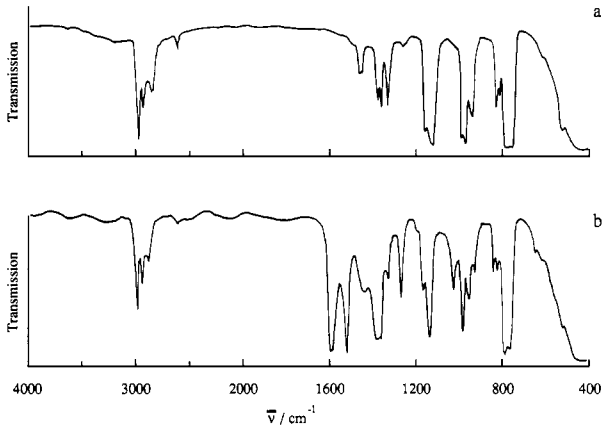

Figure 3. Infrared spectra of (a) $Ce(OPr^i)_4$ and (b) $Ce(OPr^i)_3(acac)$ in carbon tetrachloride.

dimers is strongly supported by the structure of the solid solvate ($Ce_2(OPr^i)_8\cdot 2HOPr^i$) studied by X-ray diffraction.[30,31] The three sets of Ce–O distances, observed by EXAFS, and their relative proportion (2:3:1) suggest that the solid-state building unit is preserved in solution with only small modifications of the distances. A schematic drawing of such a dimer is shown in Figure 2a. It consists of two edge-sharing distorted octahedra. The shortest Ce–O (2.13 Å) accounts for the terminal isopropoxides, and the medium one (2.32 Å) for the bridging and axial alkoxide groups. The longest one (2.82 Å) is attributed to isopropyl alcohol solvate molecules that provide a coordination number of 6 for each cerium nucleus.

Acetylacetone-Modified Cerium(IV) Isopropoxide. Figure 3 shows the infrared spectra of $Ce(OPr^i)_3(acac)$ and $Ce(OPr^i)_4$. The strong vibrations observed at 1600 and 1520 cm^{-1} in the infrared spectra of the modified species clearly indicate the chelation of the acetylacetonato groups to cerium.[33]

The Fourier transform of the EXAFS signal of $Ce(OPr^i)_{3.5}(acac)_{0.5}$ in isopropyl alcohol and the filtered EXAFS signal superimposed on the simulation are shown in parts c and d of Figure 1, respectively. Data obtained by fitting the nature, number, and distance of the neighboring atoms are reported in Table I. The cerium atom located at 3.69 Å from the absorbing center indicates the existence of oligomers. The acetylacetonato ligand is known not to bridge cations and therefore it seems more likely that the complexation with $x = 0.5$ preserves the dimeric structure without building up higher oligomers. Actually, the characteristics of the Ce–O shells agree very well with a geometry where the solvate molecule and a terminal isopropoxy group of one of the cerium of the original dimer are substituted by the acetylacetonato bidentate ligand. The precursor formula can thus be written $Ce_2(OPr^i)_7(acac),HOPr^i$. A schematic drawing of such a dimer is given in Figure 2b.

Similarly, EXAFS data for the modified precursor with $x = 1$ were fitted. Results are reported in Table I. The oligomeric nature of this precursor appears through the Ce–Ce correlation (3.71 Å). The longest Ce–O distance (2.70 Å) seems to indicate the presence of isopropyl alcohol molecules around cerium atoms. However these solvates are probably highly labile in solution and therefore do not play a key role in the functionality of the compound. From the dimeric structure of the unmodified precursor and the EXAFS results, a dimeric molecular structure (Figure 2c) where cerium atoms are 6-fold coordination can be proposed. Such a structure has already been observed in the solid state for $Sn(OPr^i)_3(acac)$.[34]

For $x = 2$, a dimeric structure, $Ce_2(OPr^i)_4(acac)_4$, has already been proposed on the basis of IR and EXAFS measurements.[35,36]

Hydrolysis of Precursors. The hydrolysis of modified precursors with x (acac/Ce mole ratio) smaller than 0.15 leads to the precipitation of an amorphous material. IR spectroscopy, chemical analysis, and thermal analysis were carried out on the precipitate after vacuum drying. They show that about 0.5 isopropoxy group/cerium atom remains in the solid state. This result is in agreement with previous studies on titanium and zirconium alkoxides. In these cases, complete removal of alkoxy groups has been shown to be extremely difficult under neutral conditions, even when hydrolysis is performed with an excess of water.[37,38]

With x between 0.15 and 1.0, hydrolysis yields colloidal suspensions. For constant cerium(IV) concentration, the turbidity is related to the amount of acetylacetone. The sols are opalescent and yellow for $x = 0.15$ and gradually change to almost clear and orange for $x \geq 0.5$. Hydrolyzed modified precursors solution with x between 0.15 and 1 and [Ce(IV)] $\approx$ 0.1 M form gels after a few weeks of aging at room temperature. Qualitatively the rate of gelation increases with the cerium(IV) concentration as expected from a simple kinetics law and appears to be maximum for $x = 0.5$. No gel was obtained for $x \geq 1$ even after months of aging.

Infrared spectra of freshly hydrolyzed acetylacetone modified precursors still exhibit the strong vibrations at 1600 and 1520 cm^{-1}, which are characteristic of acetylacetonato groups bounded to cerium atoms.[33] No evidence for free acetylacetone in solution is observed. The EXAFS results for freshly hydrolyzed $Ce(OPr^i)_{3.5}(acac)_{0.5}$ are summarized in Table I. The short Ce–O distance, related to terminal isopropoxy groups, has disappeared and the Ce–

(30) Bradley, D. C.; Holloway, H. *Can. J. Chem.* **1962**, *40*, 1176.
(31) Vaarstra, B.; Huffmann, J. C.; Gradeff, P. S.; Hubert-Pfalzgraf, L. G.; Daran, J. C.; Parraud, S.; Yunlu, K.; Caulton, K. G. *Inorg. Chem.* **1990**, *29*, 3126.
(32) Toledano, P.; Ribot, F.; Sanchez, C. *Acta Crystallogr.* **1990**, *C46*, 1419.
(33) Nakamoto, K. *Infrared and Raman Spectra of Inorganic and Coordination Compounds*; Wiley: New York, 1978.
(34) Chandler, C. D.; Fallon, A. D.; Koplick, A. J.; West, B. O. *Aust. J. Chem.* **1987**, *40*, 1427.
(35) Toledano, P.; Ribot, F.; Sanchez, C. *C. R. Acad. Sci. II* **1990**, *311*, 1315.
(36) Sanchez, C.; Toledano, P.; Ribot, F. In *Better Ceramics Through Chemistry IV*; Zelinski, B. J. J., Brinker, C. J., Clark, D. E., Ulrich, D. R., Eds.; MRS: Pittsburgh, 1990; p 47.
(37) Smit, P. M.; Van Zyl, A.; Kingon, A. I. *Mater. Chem. Phys.* **1987**, *17*, 507.
(38) Barringer, E. A.; Bowen, H. K. *Langmuir* **1985**, *1*, 414.

Table II. QELS Data for Solutions of Hydrolyzed Precursors with Different Molar Ratios acac/Ce

acac/Ce = x	[Ce(IV)], M	dilution	mean hydrodyn diam, Å
0.15	0.05	1/40	450
0.25	0.05	1/10	170
0.5	0.05	no	30
1.0	0.05	no	≈15

Table III. SAXS Data for Solutions of Hydrolyzed Precursors with Different acac/Ce Ratios

acac/Ce = x	slope	limits[a]	ρ[b]
0.15	−2.8	$-4.4 < \ln Q < -2.6$	0.999
0.25	−2.8	$-3.8 < \ln Q < -2.6$	0.998
0.50	−2.2	$-4.0 < \ln Q < -2.6$	0.999
0.75	−1.8	$-4.0 < \ln Q < -2.6$	0.998
1.00			

[a] Limits used for least-squares fitting. [b] Correlation coefficient.

Ce distance (3.80 Å) gets closer to that found in CeO_2 (3.84 Å).[39] The number of cerium neighbors stays low (1.2), indicating a very poorly ordered open structure. One may assume that hydrolysis of $Ce(OPr^i)_{3.5}(acac)_{0.5}$ yields a low weight and weakly connected oxo-polymeric species. IR spectroscopy and ^{13}C CP MAS NMR were performed on the xerogel. The vibrations at 1600 and 1520 cm^{-1} and the ^{13}C chemical shifts at 26.0 ($\underline{C}H_3COCHCO\underline{C}H_3$), 104.1 ($CH_3CO\underline{C}HCOCH_3$), and 180.0 and 190.2 ppm ($CH_3\underline{C}O$-$CH\underline{C}OCH_3$) indicate the presence of bonded acetylacetonato ligands in the dried compounds.[33,40] Chemical analysis performed on the xerogel with $x = 0.5$ give 54.3% of cerium and 10.9% of carbon. This latter amount should be only attributed to acetylacetonato ligands since no other organic species is observed by IR or ^{13}C NMR. Therefore a molar ratio acac/Ce = 0.5 can be calculated. It indicates that all the acetylacetonato ligands remain chelated to cerium after hydrolysis and condensation.

The mean hydrodynamic diameter of the freshly made sols for different acac/Ce molar ratios were determined by quasielastic light scattering. Experimental conditions and results are presented in Table II. The average size of the particles decreases when the complexation molar ratio x increases.

The small-angle X-ray scattering profiles (ln–ln) of different sols ([Ce(IV) = 0.07 M) are reported in Figure 4. For each curve, the scattered intensity has been divided by an arbitrary constant in order to spread out the different profiles. The original intensities were equal for $-2.6 < \ln Q < -2.0$. The slope of the central part of the profile was determined by least-squares fitting. The slopes, the limits and the correlation factors are listed in Table III. When the complexation ratio (x = acac/Ce) increases, the slope becomes less negative (−2.8 → −1.8). The slope obtained for $x = 0.75$ (−1.8) is between those expected for linear swollen polymers (−1.67) and swollen branched polymers (−2.0).[41] For $x = 0.5$, the slope (−2.1) is intermediate between those expected for swollen branched polymers (−2.0) and randomly branched ideal polymers (−2.3).[41] The slope of −2.8, observed for $x = 0.15$ or 0.25, still indicates a mass fractal. These slopes, which are related to the density of the objects, show that the inner structure of the scatterers changes from tenuous to more cross-linked when x decreases. On the scattering profile for $x = 0.75$, a maximum is observed for $\ln Q = -4.4$. This maximum disappears upon dilution and thus can be related to a correlation length between scatterers. The average distance ($d = 2\pi/Q$) between objects would be about 500 Å.

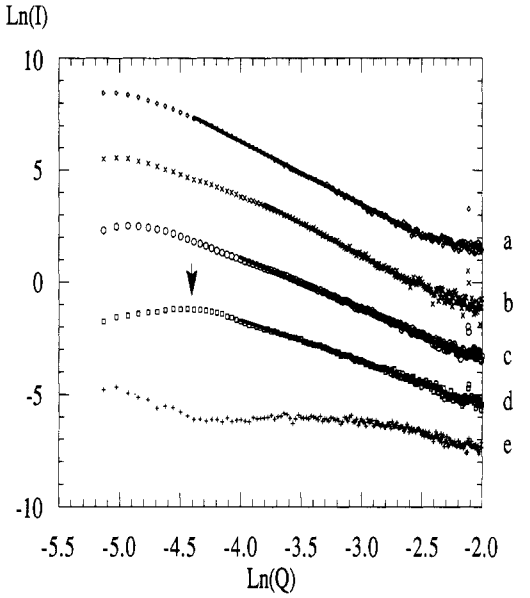

Figure 4. SAXS profiles plotted as ln I vs ln Q for various dispersions obtained by hydrolysis with $H_2O/Ce = 10$ of isopropyl alcohol solutions of $Ce(OPr^i)_{4-x}(acac)_x$: (a) $x = 0.15$; (b) $x = 0.25$; (c) $x = 0.5$; (d) $x = 0.75$; (e) $x = 1.0$.

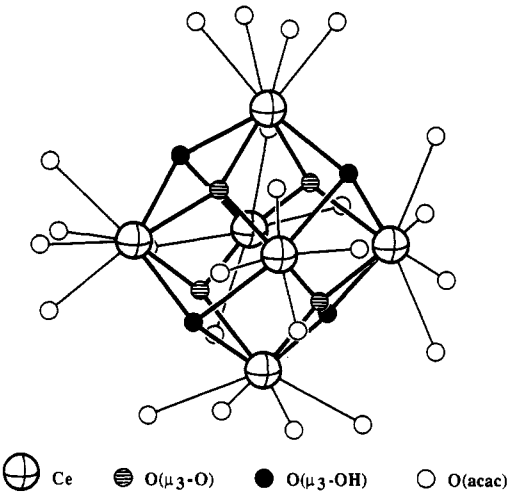

Figure 5. ORTEP drawing of $Ce_6(\mu_3\text{-}O)_4(\mu_3\text{-}OH)_4(acac)_{12}$.[35]

For $1 \le x \le 2$, SAXS and QELS measurements indicate that particles do not form. One may suggest that only molecular oligomeric compounds are obtained upon hydrolysis. These compounds are soluble but they may crystallize. It has been shown recently that the hydrolysis of $Ce(OPr^i)_2(acac)_2$ ($x = 2$) leads to the formation of a crystalline hexamer of formula $Ce_6(\mu_3\text{-}O)_4(\mu_3\text{-}OH)_4(acac)_{12}$.[35] The ORTEP drawing of this compound is presented in Figure 5.

A rough phase diagram for the hydrolysis behavior of the acetylacetone-modified cerium(IV) isopropoxide (room temperature, $H_2O/Ce = 10$, [Ce(IV)] ≈ 0.1 M and neutral conditions) is shown in Figure 6.

Model. At room temperature and without acid catalysis, hydrolysis of acetylacetonato ligands is very difficult.[15,16,42] On the other hand, alkoxy groups (isopropoxy) are quickly cleaved by water molecules. Consequently the hydrolysis

(39) *Nat. Bur. Stand. (US) Monogr.* **1983**, *20*, 38.
(40) Wilkie, C. A.; Haworth, D. T. *J. Inorg. Nucl. Chem.* **1978**, *40*, 195.
(41) Daoud, M.; Joanny, J. F. *J. Phys. (Paris)* **1981**, *42*, 1359.
(42) Sanchez, C.; Livage, J.; Henry, M.; Babonneau, F. *J. Non-Cryst. Solids* **1988**, *100*, 65.

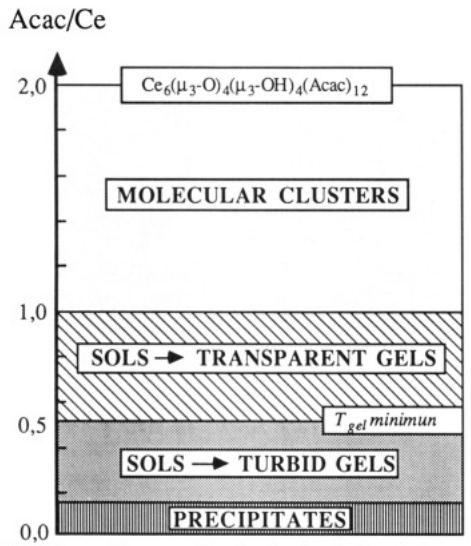

Figure 6. Phase diagram for the hydrolysis of the acetylacetone-modified cerium(IV) isopropoxide (room temperature, $H_2O/Ce = 10$, [Ce(IV)] ≈ 0.1 M, neutral conditions).

of acetylacetonato-modified precursors is strongly differentiated.[43] Such behavior is clearly illustrated by the closo-type structure (Figure 5) obtained upon hydrolysis of the modified precursor $Ce_2(OPr^i)_4(acac)_4$.[35] All the isopropoxy groups have been removed upon hydrolysis, while all the acetylacetonato ligands are still present.[35,36] Such chelating ligands play a key role. They control the spatial extension of the oxide core "$Ce_6(\mu_3\text{-}O)_4(\mu_3\text{-}OH)_4$" obtained via olation and oxolation reactions.[36,44] They also cover the surface and lead to a stabilization effect as for micels. Moreover they introduce a decoupling in hydrolysis rates, thus promoting a control of the functionality of the precursor.[43]

A simple model based on the modification of the overall functionality of the precursors with the complexation ratio x can account for the different results observed upon hydrolysis of acetylacetone-modified cerium(IV) isopropoxide precursors. According to spectroscopic characterizations, a main dimeric structure has been proposed for precursors. Such a degree of association has already been found for many acetylacetone-modified alkoxides of tetravalent metals (Zr(IV), Ti(IV), Sn(IV)).[15,34,45] Consequently the starting solutions of acetylacetone-modified cerium(IV) isopropoxide may be pictured as a mixture of the four following species: $Ce_2(OPr^i)_8{\cdot}2HOPr^i$ (I), $Ce_2(OPr^i)_7(acac){\cdot}HOPr^i$ (II), $Ce_2(OPr^i)_6(acac)_2$ (III), and $Ce_2(OPr^i)_4(acac)_4$ (IV). The proportions of the different species depend on the complexation ratio. Reactivity of each starting solutions is mainly controlled by the behavior of these four compounds upon hydrolysis. A cartoon of the different routes of synthesis of cerium oxide based materials may be proposed (Figure 7). Let us first describe the borderline of the phase diagram:

For $x = 1$ or $x = 2$, compounds III or IV are the main components in solution. Hydrolysis of isopropoxy groups is fast but condensation is strongly limited by the acetylacetonato ligands. It results in the formation of weakly condensed species that cannot bind to one another. Acetylacetonato groups act as a protecting belt that prevent the "oxo" core from further condensation. Therefore gelation cannot occur even after a long time. Molecular

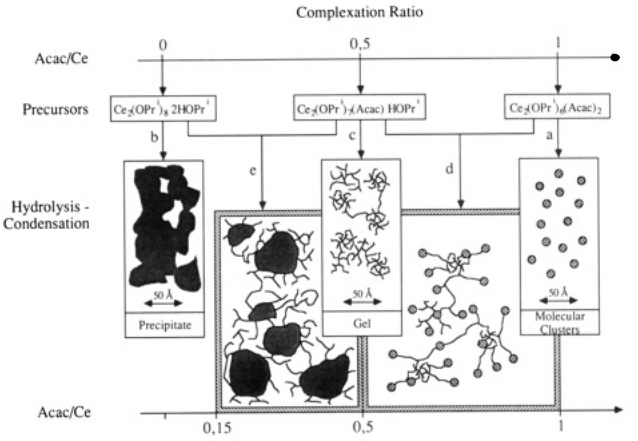

Figure 7. Schematic representation of the hydrolysis–condensation behavior of $Ce(OPr^i)_{4-x}(acac)_x$.

compounds are thus obtained. They can lead to crystalline compounds as those obtained for $x = 2$ (Figure 5) or small oligomeric amorphous species as those synthesized for $x = 1$. It is noteworthy to mention that the hydrodynamic diameter of these latter species (measured on the hydrolyzed solution of III) is about the size of the closo hexamer (Figure 5), ca. 15 Å (route a of Figure 7).

For $x = 0$, compound I is the unique component. In contrast with the previous case, both hydrolysis and condensation reactions are fast because condensation cannot be inhibited by acetylacetonato ligands. An oxide type network can extend, yielding a precipitate (route b of Figure 7).

For $x = 0.5$, compound II controls the behavior of the precursor solution. Acetylacetonato ligands which are not removed upon hydrolysis partially limit the condensation. The complexation ratio is too low to force the formation of a closo type structure. However, chelating ligands provide a sufficient decrease of the functionality of the precursor to orientate condensation reactions toward the formation of weakly branched polymeric species. Upon aging, a gel is obtained as soon as percolation of these oxo polymers is reached through slow cross-linking reactions (route c of Figure 7).

Lets now describe the intermediate regimes:

For $0.5 < x < 1$, II and III are the main components of the precursor solutions. Condensations yield also polymeric species. But hydrolyzed species coming from III whose proportion gets larger as x grows toward 1 poisoned the reactive sites. The polymers formed are therefore more tenuous as evidenced by SAXS. For similar reasons, gelation is slackened (route d of Figure 7).

For $0 < x < 0.5$, I and II are the components to be considered to understand the reactivity of the system. The isopropoxy groups of I and II are quickly removed upon hydrolysis. Actually, partial charge calculation indicates that isopropoxy groups of II should be hydrolyzed faster.[46] In contrast, the absence of acetylacetonato ligands on I gives it a better ability to condense. Therefore the system tends to behave as $x = 0$ initially and particles start to form. Hydrolyzed and partially condensed species coming from II, because of their lower functionality, terminate the growth by condensation on the outside of the particles. This phenomenon inhibits the spatial extension of the solid phase and prevents aggregation and precipitation (as long as the amount of II is high enough, ca. $x > 0.15$). This case

(43) Sanchez, C.; Livage, J. *New J. Chem.* **1990**, *14*, 513.
(44) Livage, J.; Henry, M.; Sanchez, C. *Prog. Solid State Chem.* **1988**, *18*, 259.
(45) Leaustic, A.; Babonneau, F.; Livage, J. *Chem. Mater.* **1989**, *1*, 240.
(46) Livage, J.; Henry, M. In *Ultrastructure Processing of Advanced Ceramics*; Mackenzie, J. D., Ulrich, D. R., Eds.; Wiley: New York, 1988; p 183.

is similar to the poisoning of a highly reactive process by a terminating step. One acetylacetonato ligand for every seven cerium atoms seems too low to show such an effect. But work on acetylacetone-modified titanium alkoxide shows that a acac/Ti ratio of 0.1 is enough to force the formation of closo type structure.[47] Gelation, observed for $x > 0.15$, occurs upon aging by cross-linking of the polymeric species condensed on the surface of the particles (route e of Figure 7).

Conclusions

This simple model can be extended with a few precautions, to some other metal alkoxides with d or p empty orbitals (Zr(IV), Ti(IV), Sn(IV), Al(III)) that have the tendency to form oligomeric species in solution and whose reactivity toward acetylacetone is close to those of cerium(IV) alkoxides.[15,48,49,50] The key point remains controlling the hydrolysis–condensation of alkoxide-based systems by chelated species of lower functionality.

Work by Papet et al. on hydrolysis condensation of acetylacetone-modified zirconium *n*-propoxide shows also a great influence of the acac/Zr ratio.[19] The most probable dimeric structure of the precursors leads us also to consider the species of type I (unmodified dimer), II (dimer modified with one acetylacetone, acac/Zr = 0.5), and III (dimer modified with two acetylacetone, acac/Zr = 1).[15,51] For acac/Zr = 1, III is the unique component, and no gelation is observed. Transparent monolithic gels can be obtained for only acac/Zr ≥ 0.5, where II and III are the main components. In this case, gelation time increases with acetylacetone content, ca. increasing proportion of III. Below this threshold value (x =0.5), precipitation takes place almost instantly. The resulting material is a nontransparent gel. This solidification occurs more probably because of a flocculation process induced by the high zirconium concentration (≈1 M) than from growth of polymers.

QELS experiments performed on systems where 0.3 < acac/Zr < 1 show the same trend as for modified cerium alkoxides: before gelation, the size of particles gets smaller for higher content of acetylacetone and reaches a plateau when acac/Zr ≥ 0.5.[47]

Similar variations have been observed on acetylacetone-modified titanium *n*-butoxide. QELS experiments showed that particles formed upon hydrolysis get smaller as the acac/Ti ratio increases. The mean hydrodynamic diameter varies from 20 to 400 Å when the complexation ratio changes from 1 to 0.3.[47] These results are a good indication that our model could be extended to titanium *n*-butoxide whose acetylacetone-modified products are mainly dimeric in solution.[45]

The basis of this model is the formation of complexed species that exhibit a lower functionality toward hydrolysis and condensation reactions. This decrease in functionality emerges from the fact that some of the ligands (e.g., acetylacetonato) are much less hydrolyzable than alkoxy groups. The phase diagram presented in Figure 6 shows that chemistry, via complexation, allows an almost continuous pathway between molecular clusters, colloidal solutions, gels (transparent or turbid), and precipitates. Such results should be general for many combinations of metal alkoxides–chelating ligands. Borders between domains depend, of course, on the complexing power of the chelate. For instance, for a given metal alkoxide, β-keto esters exhibit a lower complexing power than β-diketonates, suggesting that the borders of the phase diagram will move upward. For a given couple (metal alkoxide–chelating ligand) the borders of the phase diagram are also shifted by temperature and pH. This phenomenon can be illustrated by the results of De et al.[20] Fibers are drawn from solutions where acac/Zr = 1. Because of the similarities between zirconium and cerium, these solutions should give rise to only small clusters (Figure 6), which are inappropriate for fabricating fibers. Actually, the use of acid catalysis diminishes the complexation strength of acetylacetone toward zirconium and shifts upward the border between gel and molecular clusters.[15] Chemical analysis confirms this effect: De et al. found acac/Zr = 0.75 for dried fibers. According to our model, one may expect, for a complexing ratio of 0.75, the formation of branched polymers which, during aging, exhibit a viscosity high enough to draw fibers. Such branched polymers are probably a good picture to explain fiber-forming ability.[52] In contrast, De et al. have proposed a linear ladder-type polymer where zirconium atoms remain in 6-fold coordination.[20] Zirconium alkoxides should normally increase their coordination to 7 or 8 upon hydrolysis. Actually, an X-ray structural study has shown that even under very mild hydrolysis conditions ($H_2O/Zr \approx 1$), zirconium propoxide modified with 1 acetylacetonato ligand/zirconium atom forms tetramers where all the zirconium atoms are in sevenfold coordination.[51]

Acknowledgment. We thank B. Cabanes, C. Williams, and O. Lyon for X-ray scattering experiments, M. Verdaguer for help in EXAFS measurements, and A. Michalowicz for EXAFS program facilities.[28] This work was part of a Ph.D. Thesis financially supported by Rhône-Poulenc Co.

(47) In, M.; Toledano, P.; Sanchez, C., to be published.
(48) Bradley, D. C.; Mehrotra, R. C.; Gaur, D. P. *Metal Alkoxides*; Academic Press: New York, 1978.
(49) Maire, J. C. *Ann. Chim. (Paris)* **1961**, 969.
(50) Debsikdar, J. C. *J. Mater. Sci.* **1985**, *20*, 44.
(51) Toledano, P.; In, M.; Sanchez, C. *C. R. Acad. Sci. II* **1990**, *311*, 1161.
(52) Reference 13, pp 209–210.